Electrostatic Contributions to the Free Energy of Clustering of an Ionomer

Vandana K. Datye† and Philip L. Taylor*

Department of Physics, Case Western Reserve University, Cleveland, Ohio 44106.
Received August 29, 1984

ABSTRACT: Monte Carlo simulations have been performed in order to determine the electrostatic energy of an ionic cluster in an ionomer as a function of cluster size and temperature. Studies of several different types of organization of ion pairs within a cluster yield results that are not very sensitive to a variation of geometry. As the size of the cluster is increased a broad peak appears in the specific heat, indicative of a transition from a low-temperature phase in which the orientations of the ionic dipoles are ordered to one in which the orientations are disordered.

1. Introduction

Several theoretical models[1-5] have been proposed for the phenomenon of ionic clustering in ionomers. While these models have many features in common, the differences in some of the detailed assumptions may lead to consequences that are considerably different. In this paper, we examine closely one term in the free energy of clustering, namely, the electrostatic contribution. This term, which is the one primarily responsible for ionic aggregation, has been treated in a semiempirical fashion by most authors.[2-4] A first-principles calculation of the electrostatic energy is, however, fairly straightforward and was first attempted by Eisenberg.[1]

In Eisenberg's model, the electrostatic energy is described in terms of interactions between dipoles formed by the association of the fixed ions with counterions. The electrostatic energy of a cluster is then computed by assigning fixed positions and orientations to the ionic dipoles. The main drawback of this calculation is that by imposing predetermined orientations on the dipoles an important degree of freedom of the system is suppressed, and the system cannot choose the configuration that is energetically most favorable.

In an earlier paper,[5] we have reported calculations of the electrostatic energy for a spherical cluster in which the above constraint is relaxed, so that the dipoles are free to choose the orientations that minimize the electrostatic energy. This corresponds to determining the ground-state or zero-temperature electrostatic energy of a cluster. In this paper we extend our previous work to include the effect of temperature by studying the effect of thermal disorder on the electrostatic energy of the system. We have also examined two different cluster geometries, namely, spherically symmetric and cylindrically symmetric. Our calculations are most relevant to a dry, or nearly dry, membrane, where the assumption that all ions exist in association with counterions is reasonable.

The main computational tool that we have used in order to evaluate the electrostatic energy is computer simulation using the so-called Monte Carlo technique. Section 2 of this paper contains a general formulation of our model, a summary of the Monte Carlo method, and a description of the various geometries considered. In a previous paper,[6] we have commented on the connection between ionic clustering and glass temperature enhancement in ionomers. Some of the ideas presented there are further elaborated in section 3 and form a basis for discussion of the numerical results of the Monte Carlo approach.

† Present address: Biophysics Research Division, Institute of Science and Technology, University of Michigan, Ann Arbor, MI 48109.

2. Description of the Model

2.1. General Formulation. The electrostatic energy of the system arises principally from the interactions between the ion pairs, which in this calculation will be modeled as point dipoles. The electrostatic energy E_{ij} of a pair of dipoles is

$$E_{ij} = \frac{1}{4\pi\kappa\epsilon_0}\left(\frac{\vec{m}_i\cdot\vec{m}_j}{|\vec{r}_i - \vec{r}_j|^3} - \frac{3(\vec{m}_i\cdot(\vec{r}_i - \vec{r}_j))(\vec{m}_j\cdot(\vec{r}_i - \vec{r}_j))}{|\vec{r}_i - \vec{r}_j|^5}\right) \tag{2-1}$$

where $\vec{m}_i$ denotes the dipole moment of an ion pair located at $\vec{r}_i$, ϵ_0 is the permittivity of space, and κ is the dielectric constant of the medium.

The electrostatic energy of a cluster of N dipoles is then

$$E_{es}{}^N = \sum_{i<j}^{N} E_{ij} \tag{2-2}$$

The total electrostatic energy of a sample will contain both the intracluster energies listed above and also a term corresponding to intercluster interactions. Because our zero-temperature analysis has shown the lowest energy configuration to have no net dipole moment, the intercluster interactions will in general involve higher order multipole terms which are considerably smaller than the dipole–dipole term. We will therefore neglect intercluster interactions and concern ourselves with evaluating only the contribution from a single cluster.

The energy of a cluster of N dipoles located at positions $\vec{r}_i$ (in a geometry discussed in section 2.3) is

$$H_N = E_{es}{}^N + \sum_{i=1}\left(\frac{P_{\theta i}{}^2}{2I} + \frac{P_{\phi i}{}^2}{2I\sin^2\theta_i}\right) \tag{2-3}$$

where the second term on the right-hand side of (2-3) is the rotational kinetic energy of a dipole. The angles θ_i and ϕ_i are polar angles which define the orientation of a dipole relative to a fixed-coordinate system, $P_{\theta i}$ and $P_{\phi i}$ are the momenta conjugate to θ_i and ϕ_i, and I is the moment of inertia of a dipole. We will neglect vibrational motion in a dipole, since this leads to a higher order term in the dipole–dipole interaction. The total energy of a cluster will also include a term that arises owing to a conformational deformation of polymer chains on clustering, i.e., an "elastic" term. However, as pointed out earlier, in this paper we will be concerned with the electrostatic contribution alone.

All the thermodynamic quantities of interest can be obtained from the partition function of the system, defined to be

0024-9297/85/2218-1479$01.50/0

$$Z_N \propto \int_0^{2\pi} d\phi_1 \ldots d\phi_N \int_0^{\pi} d\theta_1 \ldots d\theta_N \int_{-\infty}^{\infty} dp_{\phi 1} \ldots dp_{\phi N} \int_{-\infty}^{\infty} dp_{\theta 1} \ldots dp_{\theta N} \, e^{-\beta H_N} \quad (2\text{-}4)$$

where $\beta = 1/k_B T$, and k_B is Boltzmann's constant, and T is the temperature of the system.

Integrating over the momenta in eq 2-4 we find

$$Z_N \propto \left(\frac{2\pi I}{\beta}\right)^N \int_0^{2\pi} d\phi_1 \ldots d\phi_N \int_0^{\pi} \sin\theta_1 \, d\theta_1 \ldots \sin\theta_N \, d\theta_N \, e^{-\beta E_{es}^N} \quad (2\text{-}5)$$

The partition function thus separates into a kinetic and a potential energy term

$$Z_N \propto Z_{kin} Z_{pot} \quad (2\text{-}6)$$

where Z_{pot} is the integral on the right-hand side of eq 2-5, which involves potential energy terms of the form (2-1).

The total energy of the system as a function of temperature is

$$U = -\frac{\partial \ln Z_N}{\partial \beta} = N k_B T - \frac{\partial \ln Z_{pot}}{\partial \beta} \quad (2\text{-}7)$$

In this paper we are primarily interested in evaluating the average electrostatic potential energy per dipole as a function of temperature, a quantity which we will denote by $\epsilon_{es}(T) \equiv -N^{-1}(\partial \ln Z_{pot}/\partial\beta)$. The integrations in eq 2-5 have resisted attempts at analytical evaluation; we have therefore carried out Monte Carlo computer simulations, which are described in section 2.2.

It is useful to evaluate the above quantities in the limit where we have only two dipoles in the system. Choosing the axis to lie along the line joining the two dipoles, we find

$$E_{12} = \frac{1}{4\pi\kappa\epsilon_0} \frac{m_1 m_2}{r^3} (\sin\theta_1 \sin\theta_2 \cos(\phi_1 - \phi_2) - 2\cos\theta_1 \cos\theta_2) \quad (2\text{-}8)$$

where $r = |\vec{r}_1 - \vec{r}_2|$. In the high-temperature limit, $\beta m_1 m_2/(4\pi\epsilon_0 r^3) \ll 1$, we can expand the exponential in eq 2-4, and it is easy to evaluate the partition function. In this limit

$$Z_{pot} = (4\pi)^2 \left\{1 + \frac{\beta^2 m_1^2 m_2^2}{3(4\pi\kappa\epsilon_0)^2 r^6} + \text{higher order terms}\right\} \quad (2\text{-}9)$$

and

$$\epsilon_{es}(T) = -\frac{1}{2}\frac{\phi \ln Z_{pot}}{\phi\beta} = -\frac{\beta m_1^2 m_2^2}{3(4\pi\kappa\epsilon_0)^2 r^6} \quad (2\text{-}10)$$

We see from (2-10) that even at high temperatures, the dipole–dipole interaction is attractive: this is the classical or Keesom component of the van der Waals force. Some tendency to clustering is thus always present.

The question of interest in the present case concerns the dependence of this high-temperature contribution on the size of the cluster. The short range of the van der Waals force would suggest that in the absence of collective behavior, the energy per dipole would rapidly saturate as N became greater than about 10. An electrostatic energy per dipole that continued to increase with N at a particular temperature would suggest the continued presence of collective behavior.

2.2. Summary of the Monte Carlo Method. This method is an efficient way of sampling the phase space of the system in order to determine various thermodynamic quantities of interest. The procedure we have followed is an adaptation of the Metropolis[7,8] algorithm for a system such as the Heisenberg ferromagnet[9] in which the spins have continuous symmetry. The aim of the computer simulation is to select the "most probable" states in phase space at a given temperature T. The essential steps of the simulation are as follows. Initially, random orientations are assigned to the N dipoles in a cluster; i.e., the variables ϕ_i and $\cos\theta_i$ are chosen at random from their respective ranges, $\phi_i \in [0, 2\pi]$ and $\cos\theta_i \in [-1, 1]$. This corresponds to one point in phase space. The electrostatic energy E_{es} of the cluster is computed. Next, the orientation of one dipole, say $i = 1$, is changed to another random orientation and the new energy E_{es}' computed. If $\Delta E = E_{es}' - E_{es} < 0$, the change in orientation is preserved. If $\Delta E > 0$, a random number η is chosen in the interval [0, 1]. If $\eta < e^{-\Delta E/k_B T}$ the change is preserved, whereas if $\eta > e^{-\Delta E/k_B T}$ then dipole i is returned to its initial orientation. After this procedure is carried out for the entire cluster, the final orientations of the N dipoles are taken to constitute the next point in phase space. This method reduces correlations between successive points while generating points in phase space with the appropriate Boltzmann weight.[10] Thermodynamic averages can then be taken as simple arithmetic averages over the ensemble. For example

$$\epsilon_{es}(T) = \frac{1}{M}\sum_{k=1}^{M} \frac{E_{es}^k}{N} \quad (2\text{-}11)$$

where M is the number of points in phase space generated by the Monte Carlo algorithm. Ideally M is a very large number.

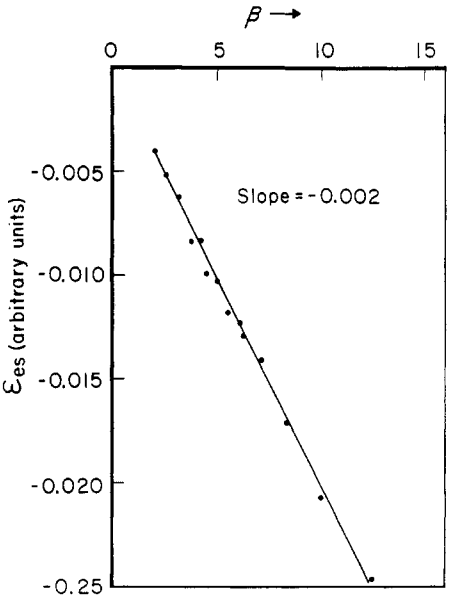

Figure 1. Electrostatic energy per dipole as a function of β for two dipoles in the high-temperature limit.

As a check on our Monte Carlo program we compare the Monte Carlo estimate for $\epsilon_{es}(T)$ for a cluster of two dipoles with the high-temperature limit obtained analytically in section 2.1. Figure 1 is a plot of $\epsilon_{es}(T)$ (in arbitrary units) from the Monte Carlo simulation for $m_1 = m_2 = 1$, $\kappa = 1$, $\epsilon_0 = 1$, and $r = 1$. We obtain a straight line with a slope of 0.002, which compares well with the value of $1/(48\pi^2)$ from eq 2-10.

2.3. Geometry of a Cluster. While experiments[11] indicate the existence of ionic clusters in an ionomer, the locations of ions within a cluster have not been unambiguously determined. We have therefore carried out

simulations assuming two alternative geometries for the organization of ions within a cluster. The intracluster geometries that we have studied are described below.

(a) Spherical Cluster. This geometry was described in an earlier paper[5] and assumes that ionic dipoles are distributed uniformly over the surface of a spherical cluster. This geometry is motivated by the inverted micelle model proposed by Gierke.[12] We assume that the dipoles form a close-packed arrangement on the surface of a cluster, the nearest-neighbor distance being determined by a molecular pair potential. While a uniform distribution is only exactly realizable for certain numbers of dipoles, a fact related to the limited number of regular polyhedra, approximately uniform distributions are readily constructed. Because all dipoles are equivalent when located on a spherical surface at points corresponding to the vertices, centers of the faces, or the midpoints of the edges of a tetrahedron, cube, octahedron, dodecahedron, or icosahedron, one may place 4, 6, 8, 12, 20, or 30 uniformly on a spherical surface. Arrays of nearly equivalent points may be constructed by repeated centering of the faces of the various polyhedra, generating approximately uniform distributions of 42, 80, 120, and 162 points.

(b) Cylindrical Clusters. This geometry is motivated by the observations of Yeager and co-workers.[13] In the cylindrical arrangement the distance between nearest-neighbor dipoles is maintained at the same value used in case a. The base of the cylinder is assumed to be a square with four dipoles placed at the vertices. The cylinder is then constructed by stacking planes of dipoles such that the nearest-neighbor distance along the axis of the cylinder equals the in-plane nearest-neighbor distance. Configurations were studied in which dipoles in alternate planes were eclipsed or staggered. The largest cluster studied consisted of 80 dipoles.

The cases considered above are clearly simplifying approximations, since in a real system some degree of randomness is to be expected. However, we do not expect this to alter significantly our results. It is also possible that there may be a volume distribution of dipoles within a cluster. While the arrangement of dipoles in the smaller spherical clusters that we have studied is not too different from a close-packed volume distribution, for larger clusters the effect of a volume distribution of dipoles could significantly modify our results.

3. Results

The parameters entering our model are (a) the dielectric constant κ, which depends on the polarizability of the intervening medium, (b) the dipole moment m of an ion pair, and (c) the nearest-neighbor distance between dipoles, which defines the fundamental length scale in the system. For concreteness, we will report numerical results for an ionomer of the Nafion type, which consists of a PTFE matrix in which the fixed ions are SO_3^- and the counterions are typically Na^+. The ionic radii of these ions are 0.24 and 0.097 nm, respectively, which leads to an ionic dipole moment of 5.4×10^{-29} C m. The dielectric constant κ will be assumed to have the same value as in bulk PTFE, i.e., $\kappa = 4$. The only free parameter that then remains to be defined in the model is the nearest-neighbor distance between dipoles. To this quantity we will assign the reasonable but somewhat arbitrary value of 1 nm, which corresponds roughly to the width of a polymer chain plus the sum of the ionic radii of the fixed ion and counterion.

3.1. Electrostatic Energy as a Function of Temperature and Cluster Size. Figure 2 is a plot of the electrostatic energy per dipole $\epsilon_{es}(T)$ as a function of temperature for spherical clusters. The different curves correspond to various numbers N of dipoles in a cluster. Also plotted on the figure for comparison is the negative of the rotational kinetic energy per dipole, k_BT. We see that the binding energy per dipole $-\epsilon_{es}(T)$ increases with cluster size. We have suggested in ref 6 that the electrostatic binding of a cluster may be responsible for glass temperature enhancement in ionomers. As we can see from Figure 2, we expect cluster size to be important in this effect, a result argued from a ground-state ($T = 0$) calculation in our earlier paper.

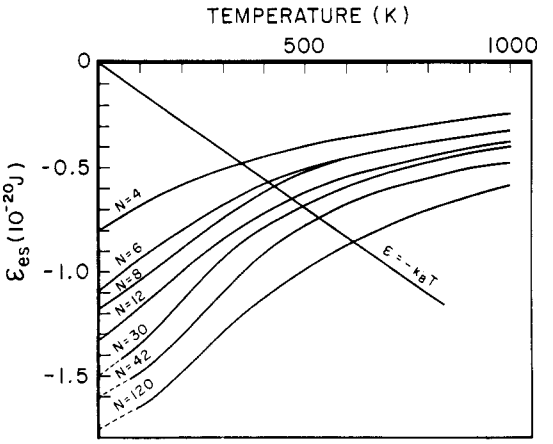

Figure 2. Electrostatic energy per dipole as a function of temperature for varying cluster size N.

At very low temperatures there is scatter in the Monte Carlo data because the system is susceptible to being locked into metastable states. This becomes more pronounced as the cluster size increases, and so the Monte Carlo data are not very useful in the low-temperature limit. We have therefore not presented data in this limit for clusters having $N \geq 30$. Instead, in Figure 2, we indicate the expected low-temperature classical behavior by a dashed line that interpolates between the Monte Carlo data at higher temperatures and the ground-state energy obtained by an independent energy minimization procedure.[5] The fact that ϵ_{es} still depends strongly on N even for $N > 40$ and $T > 1000$ K shows the importance of collective effects.

An interesting feature of Figure 2 is the curvature of the plots of ϵ_{es} vs. T. When N is small these curves are concave downward for all T. However, as N increases the curves remain concave downward at high temperatures but become concave upward at low temperatures. The point of inflection of the curve corresponds to a maximum in the specific heat C_v ($=\partial\epsilon_{es}/\partial T$). We note that the peak in the specific heat will be more pronounced than is evident from Figure 2. The classical result is not a good approximation in the low-temperature limit since one expects the specific heat to vanish in this limit as a result of quantum behavior. The hump in the specific heat may be interpreted as a glass transition peak. If, as the cluster size increases, this peak becomes sharper until, in the thermodynamic limit, a singularity occurs in the specific heat, then a phase transition would be occurring. In the low-temperature phase the orientations of the dipoles would be ordered while in the high-temperature phase the orientations would be disordered. We have carried out simulations on clusters containing as many as 120 dipoles, the main limitation in studying larger clusters being the excessive amounts of computer time required.

3.2. Effect of Geometry. Figure 3 shows the ground-state electrostatic energy of the cylindrical clusters described in section 2.3b as a function of cluster size. Also shown for comparison are the corresponding values for

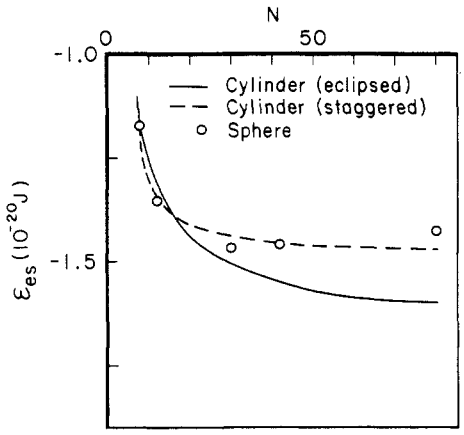

Figure 3. Ground-state electrostatic energy as a function of cluster size for cylindrical and spherical clusters.

spherical clusters. We see that the electrostatic energy does not vary significantly from one geometry to another.

3.3. Discussion. In order to have a complete theory of ionic clustering, or self-organization in ionomers, the first-principles treatment of the electrostatic term presented above has to be combined with a model for the deformation of polymer chains on clustering that contributes an elastic term to the Hamiltonian. Models for the elastic term that have been presented by us[5] and by other authors[1-4] either model polymer chains as a Gaussian random walk or else use concepts of bulk elasticity. While both approaches are reasonable as a starting point, neither is satisfactory as a theory of ionic clustering. We have therefore not attempted to combine the above model with an approximate elastic model but hope to present a more fundamental model for the elastic term based on self-avoiding random walks[14] in the near future.

Acknowledgment. This work was supported by NSF Grant CPE 81-151115. We are grateful to Dr. R. Petschek for many helpful comments.

References and Notes

(1) A. Eisenberg, *Macromolecules*, **3** (2), 147 (1970).
(2) K. A. Mauritz, C. J. Hora, and A. J. Hopfinger, in *Adv. Chem. Ser.*, **No. 187**, 183 (1980).
(3) W. Y. Hsu and T. D. Gierke, *J. Membrane Sci.*, **13**, 307 (1983).
(4) W. C. Forsman, W. J. MacKnight, and J. S. Higgins, *Macromolecules*, **17**, 490 (1984).
(5) V. K. Datye, P. L. Taylor, and A. J. Hopfinger, *Macromolecules*, **17**, 1704 (1984).
(6) V. K. Datye and P. L. Taylor, *Macromolecules*, **17**, 1414 (1984).
(7) N. Metropolis, A. W. Rosenbluth, N. M. Rosenbluth, A. H. Teller, and E. Teller, *J. Chem. Phys.*, **21**, 1087 (1953).
(8) K. Binder, Ed., *Top. Curr. Phys.*, **7** (1979).
(9) K. Binder, in *Phase Transitions Crit. Phenom.*, **56**, 1 (1976).
(10) For a proof of this result, see L. D. Fosdick, in *Methods Comput. Phys.*, 1 (1963).
(11) A. Eisenberg and H. L. Yeager, Ed., *ACS Symp. Ser.*, **No. 180** (1982).
(12) T. D. Gierke, 152nd Meeting of the Electrochemical Society, Extended Abstracts, Atlanta, GA, 1977, Abstract No. 438; *J. Electrochem. Soc.*, **124**, 319C (1977).
(13) H. L. Yeager, Z. Twardowski, and L. M. Clarke, *J. Electrochem. Soc.*, **129**, 324 (1982).
(14) P.-G. de Gennes, "Scaling Concepts in Polymer Physics", Cornell University Press, Ithaca, NY, 1979.

Nitrogen-15 Nuclear Magnetic Resonance of Cured Urea–Formaldehyde Resins Using Cross Polarization and Magic-Angle Spinning

I-Ssuer Chuang, Bruce L. Hawkins, and Gary E. Maciel*

Department of Chemistry, Colorado State University, Fort Collins, Colorado 80523

George E. Myers

Forest Products Laboratory, U.S. Department of Agriculture, Madison, Wisconsin 53705.
Received July 11, 1984

ABSTRACT: ^{15}N NMR spectra have been obtained on two urea–formaldehyde (UF) resins that were prepared with ^{15}N enriched to 99% and on model compounds with ^{15}N in natural abundance. Solid-sample techniques were used, with cross polarization (CP) and magic-angle spinning (MAS). The spectra consist largely of peaks in two partially overlapping regions. Distinctions between secondary and tertiary amide nitrogens are made partly on the basis of chemical shift differences and partly on the basis of interrupted-decoupling experiments. Overall, a lower level of structural detail is obtained than what is provided by corresponding ^{13}C CP/MAS experiments, but ^{15}N data should provide a useful supplement to ^{13}C data in the elucidation of structure in cured UF resins.

Introduction

Urea–formaldehyde (UF) resins are important binder products, especially for the manufacture of composition board, but emission of formaldehyde from UF-bonded particle board has generated concern in the particleboard industry.[1-8] For cured UF resins, both poor durability in high-temperature, high-humidity environments and the emission of formaldehyde are due to a considerable degree to hydrolytic instability,[2,9-12] which in turn is determined by the structural moieties present in the resins. Therefore, it is of considerable importance to have reliable spectroscopic techniques for determining the correlations between molecular structures and macroscopic properties of cured resins.

Four potentially reactive centers (atomic sites) in urea and two in formaldehyde are responsible for the large variety of likely structural moieties in UF resins. The following reactions are believed to occur to varying extents

0024-9297/85/2218-1482$01.50/0